Oxygen dependence of the crystal structure of $HgBa_2CuO_{4+\delta}$ and its relation to superconductivity

Q. Huang and J. W. Lynn
Reactor Radiation Division, National Institute of Standards and Technology, Gaithersburg, Maryland 20899 and University of Maryland, College Park, Maryland 20742

Q. Xiong and C. W. Chu
Texas Center for Superconductivity, University of Houston, Houston, Texas 77204

(Received 8 December 1994)

Powder neutron-diffraction profile refinement techniques have been used to investigate the oxygen dependence of the crystal structure and its effect on the superconducting phase transition in high-quality samples of the superconductor $HgBa_2CuO_{4+\delta}$ ($0.04 \leq \delta \leq 0.23$). The system remains tetragonal (space group $P4/mmm$) over the full range of temperature (10–300 K) and oxygen concentration explored. The a-axis lattice parameter decreases smoothly with increasing δ, while the c-axis lattice parameter exhibits a maximum. The extra oxygen in the material is found to randomly occupy the centered O(3) site ($\frac{1}{2}$, $\frac{1}{2}$, 0) in the Hg layer, and no other additional site for the extra oxygen was found in the structure. There is also no mixing of the cations on the Cu and Hg sites. T_c is observed to vary strongly with δ, increasing from 0 K for $\delta=0.04$ to a maximum $T_c=95$ K at $\delta \cong 0.18$, and then decreasing rapidly for larger δ. The relationship of $T_c(\delta)$ to the rate of hole doping on the CuO_2 planes indicates that this doping level is only half of that expected for O^{2-} ions. Our structural studies reveal an interesting correlation between the occupation of the O(3) site and the movement of the Ba ions towards the O(3) and away from the Cu-O planes. The Ba layer thus becomes structurally disordered, and this disorder is found to closely mirror the $T_c(\delta)$ behavior. Valence and/or distance arguments for the O(3) then suggest that this oxygen is only singly ionized.

INTRODUCTION

The new mercury superconductors of formula $HgBa_2Ca_{n-1}Cu_nO_{2n+2+\delta}$ have generated considerable interest in the superconductivity community because of the high transition temperatures associated with these compounds.[1–14] In particular, the single layer ($n=1$) material (designated Hg1201) has the highest superconducting transition temperature of any one-layer cuprate, with $T_c=95$ K. T_c is found to initially increase with the number of layers in the unit cell (analogous to the Tl and Bi series of materials), with $T_c=126$ K for $n=2$ (Hg1212) and 135 K (Hg1223) for $n=3$. In addition, these transition temperatures increase with the application of pressure, saturating at 118, 154, and 164 K for $n=1,2,3$, respectively.[13] The fourth member (Hg1234) has also been synthesized,[11] with a somewhat lower T_c of 126 K, while T_c is found to decrease to 101 K for the five Cu-layer system (Hg1245).[14]

All the compounds belonging to this series of materials have the same tetragonal $P4/mmm$ symmetry, with lattice parameters given approximately by $a \approx 3.85$ Å, and $c \approx 9.5+3.2(n-1)$ Å. Their structures consist of a simple stacking of layers:

$n=1$: $[(HgO_\delta)_o(BaO)_c(CuO_2)_o(BaO)_c](HgO_\delta)_o\ldots$

$n=2$: $[(HgO_\delta)_o(BaO)_c(CuO_2)_o(Ca)_c(CuO_2)_o(BaO)_c](HgO_\delta)_o\ldots$

$n=3$: $[(HgO_\delta)_o(BaO)_c(CuO_2)_o(Ca)_c(CuO_2)_o(Ca)_c(CuO_2)_o(BaO)_c](HgO_\delta)_o\ldots$,

etc., where the square brackets include the contents of one unit cell and the subscripts c and o indicate that the cations are at the center or the origin of each layer, respectively. The extra oxygen present in these compounds, which causes the electrical doping, is found to be located on the centered position of the Hg plane at the $\frac{1}{2},\frac{1}{2},0$ site. In the first member of the homologous series, Hg1201, the copper has a very elongated octahedral coordination,[3,4] while in the high-layer members it has fivefold pyramidal or fourfold square-planar coordination depending in which layer the Cu resides.[9,12] In all cases the apical Cu-O distances along the c axis are significantly larger than the Cu-O distances in the planes perpendicular to c. Moreover, the oxygen atoms located on the

(CuO_2) layer are coplanar, or almost coplanar, with the copper atoms, in contrast to other superconductors such as $YBa_2Cu_3O_7$ where the (CuO_2) planes are significantly buckled.

The simplest Hg material from a structural point of view is, of course, the single-layer $HgBa_2CuO_{4+\delta}$ system, and we have therefore undertaken a detailed study of the crystallography as a function of oxygen doping to elucidate the relationship between the structure and superconducting properties. The crystal structure of $HgBa_2CuO_{4+\delta}$ has already been analyzed in some detail via neutron powder diffraction by Wagner *et al.*[3] and by Chmaissem *et al.*[4] In the study by Wagner *et al.*[3] it was suggested that some of the Cu substitutes onto the Hg sites, with a correlation between this Cu substitution and the oxygen doping in the Hg layer. However, Chmaissem *et al.*,[4] as well as the present results on more phase-pure samples, show that there is no mixing of the cations within experimental error. Recent studies of the effect of oxygen doping on the T_c for Hg1201 suggest, though, that there may be two kinds of oxygen-doping sites in the material.[15] In order to address this question as well as to clarify the relationship between the superconductivity and the crystal structure, we have prepared high-quality samples of $HgBa_2CuO_{4+\delta}$ and have used powder neutron diffraction to analyze the structure of the compounds as a function of doping δ. We have not been able to identify a second oxygen site, but we have found a direct structural correlation between the doped oxygen and the Ba ions, which mirrors the behavior of $T_c(\delta)$.

EXPERIMENTAL PROCEDURES

The powder samples of $HgBa_2CuO_{4+\delta}$ were prepared for the neutron powder diffraction studies by using the solid-state reaction technique described by Meng *et al.*[16] The heat-treatment conditions of the specimens are listed in Table I. The sample labeled *S*1 was used to obtain most of the diffraction data. In each case the sample was prepared and/or heat treated to obtain a particular oxygen concentration. The sample was then characterized by both x-ray-diffraction and magnetic-susceptibility measurements. The observed onset superconducting transition temperatures are also shown in Table I; further details of the superconducting properties and measurements of these samples can be found elsewhere.[15] The neutron-diffraction data were then obtained and analyzed, before the sample was further heat treated to investigate a different oxygen concentration. A second sample was prepared and annealed for the final measurement, and is designated *S*2.

TABLE I. Heat treatment conditions of $HgBa_2CuO_{4+\delta}$.

Sample no.	Label	Heat treatment	T_c (K)	δ
1	*S*1-AP	As-prepared	95	0.18(1)
	*S*1-AV	Annealed in vacuum	53	0.08(1)
	*S*1-RAO	Reannealed in oxygen	94	0.18(1)
	*S*1-RAV	Reannealed in vacuum	0	0.04(1)
	*S*1-RAOHP	Reannealed in oxygen under high pressure	30	0.23(1)
2	*S*2-PHP	Prepared in oxygen under high pressure	80	0.21(1)

Neutron powder-diffraction data were collected using the 32-detector high-resolution powder diffractometer located at the Research Reactor of the National Institute of Standards and Technology. The Cu(311) monochromator was employed at a wavelength of 1.539(1) Å. The horizontal collimations used were 15′, 20′, and 7′ (full-width-at-half maximum) before and after the monochromator, respectively, and after the sample. A cylindrical vanadium sample holder was used to hold the powder, which was then mounted in a He refrigerator to control the temperature.

The structural refinements were carried out with the general structure analysis system (GSAS) program of Larson and Von Dreele[17] using the intensity data in the 2θ range from 8 to 145°. Neutron-scattering amplitudes used in the refinements were 1.266, 0.525, 0.772, and 0.581 (10^{-12} cm) for Hg, Ba, Cu, and O, respectively.[17] All the observed peaks in the diffraction pattern were accounted for by the expected Hg1201 structure, with the exception of two whose intensities were less than 1.5% of the strongest peak. The small impurity content attests to the high quality of the samples. There was a significant amount of nuclear absorption by the Hg, and thus the values of μR were determined experimentally for each sample. They ranged from 0.34–0.52, and the intensity data were then corrected for absorption in the standard way.[17]

The initial refinement in each case was carried out assuming the symmetry of space group $P4/mmm$ and using as starting parameters those given by Chmaissem *et al.*[4] The occupancy factors for the extra oxygen atoms O(3) located at $(\frac{1}{2},\frac{1}{2},0)$ on the (HgO_δ) layer were refined with the other parameters, keeping the thermal factor B[O(3)] fixed. The value of n[O(3)] obtained in this calculation was 0.18 for the as-prepared sample ($T_c=95$ K), which is significantly higher than the values of 0.1 and 0.063 reported in the previous publications for as-prepared samples.[3,4] Since the temperature parameter and occupancy factor can sometimes be highly correlated, refinements were also carried out over a wide range of values for B[O(3)], varying from 0.1 to 3.2 Å^2. The corresponding values of n[O(3)] only changed from 0.15(1) to 0.21(1), confirming that the amount of extra oxygen in the as-prepared sample used in our experiment is about 0.18 atoms per formula unit. Refinements in which the occupancies of Hg, Ba, and Cu were varied showed that the amounts of those metals in the structure were not statistically different from the assumed nominal stoichiometry [n(Hg)=0.99(2), n(Ba)=1.07(2), and n(Cu)=1.06(2)]. Attempts to refine the occupancy of the oxygen on the $(\frac{1}{2},0,z)$ site gave a value of $n=-0.008(8)$, indicating that this position is completely empty, in agreement with the results of Chmaissem *et al.*[4] The same refinement procedures were used for the other samples and for the data collected at each temperature. In addition, for the overdoped samples recent Raman and

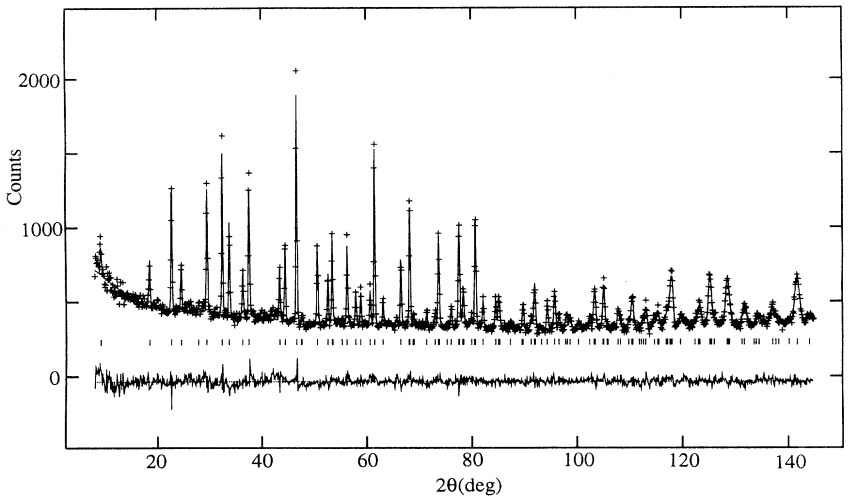

FIG. 1. Rietveld refinement profile of the neutron powder-diffraction data obtained on the as-prepared sample of $HgBa_2CuO_{4+\delta}$ at 296 K. The observed data are represented by the points (+), and the refinement by the solid curve. The positions of the Bragg peaks are also indicated. The difference between the observations and the calculated profile is shown at the bottom of the figure.

differential thermogravimetric analysis data suggest that there may be another oxygen site in this compound,[18] in particular at the (x,x,z) or $(\frac{1}{2},\frac{1}{2},z)$ sites. Refinements were thus also carried out with oxygen occupancy parameters at these sites, but no statistically significant occupancy was observed.

In the final refinement for each (δ, T), the occupancies of all atoms except the O(3) site were kept fixed at their stoichiometric values (except as discussed below). Figure 1 shows the room-temperature diffraction pattern obtained on the as-prepared sample. The difference between the refinement and the observations is shown at the bottom, and we see that the model provides an excellent representation of the data. The only impurity peaks found in the pattern occur at $2\theta \sim 20°$ and 42°, and the phase producing these peaks has not been identified. The results of these refinements are presented in Table II and the relevant bond distances are listed in Table III.

RESULTS AND DISCUSSION

We first consider the basic features and general trends of the structure of $HgBa_2CuO_{4+\delta}$, shown schematically in Fig. 2, as a function of oxygen doping (and temperature). As noted earlier, the copper atoms are coordinated by six oxygen atoms which form a very elongated octahedron, with a Cu-O(2) apical distance of 2.78 Å and a Cu-O(1) in-plane distance of 1.94 Å (at 296 K). In the stoichiometric compound the Ba ions are eightfold coordinated, by four O(1) and four O(2) atoms. This coordination becomes ninefold when O(3) is present and the coordination polyhedron can be considered to be a capped cubo-octahedron. The number of Ba atoms with ninefold coordination depends of course on the O(3) content δ. The coordination of the Hg ions also depends on how the O(3) are distributed in the plane (HgO_δ), as shown in Fig. 3. If locally all the $\frac{1}{2},\frac{1}{2},0$ sites are empty the mercury will have twofold coordination via the O(2) sites along the c axis, while if they are all occupied it will have sixfold octahedral coordination. For intermediate cases, different kinds of coordination are possible: If only one of the positions (A, B, C, or D) is occupied then the Hg atom in the center is threefold coordinated, if two are occupied we have either square-planar ($A+B$ or $C+B$) or tetrahedral ($A+B$, $A+C$, etc.) coordination, and finally, if any three of the possible positions are occupied the polyhedron will be a fivefold pyramid.

Figure 4 shows the variation of the lattice parameters and bond distances of the as-prepared sample as a function of temperature; similar results are obtained for the other values of δ. The a and c lattice parameters decrease

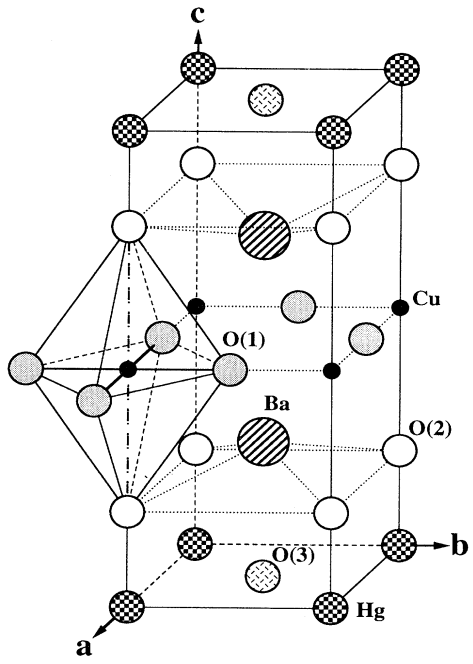

FIG. 2. Crystal structure of $HgBa_2CuO_{4+\delta}$. The doping occurs on the partially occupied O(3) site.

TABLE II. Structural parameters for $HgBa_2CuO_{4+\delta}$. Space group: $P4/mmm$. Atoms position: Hg: $1a(0,0,0)$, Ba: $2h(\frac{1}{2},\frac{1}{2},z)$, Cu: $1b(0,0,\frac{1}{2})$, O(1): $2e(0,\frac{1}{2},\frac{1}{2})$, O(2): $2g(0,0,z)$, O(3): $1c(\frac{1}{2},\frac{1}{2},0)$. Full occupancy for Hg, Ba, Cu, O(1), and O(2).

Sample label [T_c (K)]		*S*1-AP (95)				*S*1-AV (53)		*S*1-RAO (94)	*S*1-RAV (0)	*S*1-RAOHP (30)	*S*2-PHP (80)
Data collected at		296 K	150 K	80 K	10 K	296 K	10 K	295 K	295 K	295 K	295 K
	a (Å)	3.880 51(7)	3.874 36(7)	3.872 26(7)	3.871 43(6)	3.892 76(9)	3.883 92(7)	3.880 62(8)	3.895 54(9)	3.875 13(8)	3.876 2(1)
	c (Å)	9.528 8(3)	9.511 4(2)	9.504 5(2)	9.502 3(2)	9.545 1(3)	9.519 2(3)	9.527 9(3)	9.533 1(3)	9.517 5(3)	9.521 7(4)
	V (Å^3)	143.487(7)	142.772(6)	142.515(6)	142.420(6)	144.642(9)	143.596(6)	143.483(8)	144.668(8)	142.920(8)	143.06(1)
Hg	B (Å^2)	1.37(5)	0.94(4)	0.77(4)	0.53(4)	1.29(5)	0.43(4)	1.41(5)	1.23(4)	1.46(5)	1.24(5)
Ba	z	0.298 1(3)	0.298 3(3)	0.298 1(5)	0.298 6(3)	0.302 5(4)	0.302 3(3)	0.298 8(5)	0.302 6(3)	0.295 8(3)	0.297 1(4)
	B (Å^2)	0.80(5)	0.48(4)	0.42(4)	0.30(4)	0.73(5)	0.39(4)	0.88(5)	0.83(5)	0.74(5)	0.77(6)
Cu	B (Å^2)	0.59(5)	0.34(5)	0.20(5)	0.21(5)	0.59(5)	0.18(4)	0.56(5)	0.56(5)	0.50(5)	0.34(5)
O(1)	B (Å^2)	0.82(5)	0.50(5)	0.52(5)	0.37(5)	0.64(5)	0.38(4)	0.75(5)	0.72(5)	0.58(5)	0.57(6)
O(2)	z	0.207 6(3)	0.208 2(3)	0.208 2(3)	0.208 8(3)	0.206 6(3)	0.207 7(3)	0.207 4(3)	0.206 3(3)	0.209 3(3)	0.208 0(3)
	B (Å^2)	1.42(5)	1.04(5)	0.72(5)	0.58(5)	1.51(6)	0.59(5)	1.35(5)	1.51(6)	1.37(5)	1.30(6)
O(3)	B (Å^2)	1.6	1.0	0.8	0.5	1.6	0.5	1.6	1.6	1.6	1.6
	n	0.18(1)	0.18(1)	0.18(1)	0.19(1)	0.08(1)	0.09(1)	0.18(1)	0.04(1)	0.23(1)	0.21(1)
	R_p (%)	5.84	6.32	6.50	6.50	6.90	7.15	6.50	5.67	4.01	5.05
	R_{wp} (%)	6.87	7.50	7.77	7.87	8.26	8.81	7.71	6.97	4.82	6.47
	χ^2	1.13	1.10	1.17	1.11	1.20	1.41	1.24	1.38	1.02	1.72

TABLE III. Selected bond distances (Å) of $HgBa_2CuO_{4+\delta}$.

Sample label [T_c (K)]		*S*1-AP (95)				*S*1-AV (53)		*S*1-RAO (94)	*S*1-RAV (0)	*S*1-RAOHP (30)	*S*2-PHP (80)
Data collected at		296 K	150 K	80 K	10 K	296 K	10 K	295 K	295 K	295 K	295 K
Hg-O(2)	×2	1.978(3)	1.980(3)	1.979(3)	1.984(3)	1.972(3)	1.977(3)	1.976(3)	1.967(3)	1.992(3)	1.981(3)
Hg-O(3)	×δ	2.743 93(5)	2.739 59(5)	2.738 10(5)	2.737 52(5)	2.752 60(7)	2.746 35(5)	2.744 01(6)	2.754 57(6)	2.740 13(5)	2.740 89(7)
Cu-O(1)	×4	1.940 25(4)	1.937 18(3)	1.936 13(3)	1.935 72(3)	1.946 38(5)	1.941 96(4)	1.940 31(4)	1.947 77(4)	1.937 56(4)	1.938 10(5)
Cu-O(2)	×2	2.786(3)	2.777(3)	2.773(3)	2.767(3)	2.793(3)	2.783(3)	2.788(3)	2.780(3)	2.767(3)	2.780(3)
Ba-O(1)	×4	2.733(2)	2.726(2)	2.726(2)	2.722(2)	2.709(2)	2.704(4)	2.726(2)	2.708(2)	2.744(2)	2.736(2)
Ba-O(2)	×4	2.876(1)	2.871(1)	2.868(1)	2.868(1)	2.901(2)	2.890(1)	2.879(2)	2.903(1)	2.861(1)	2.869(1)
Ba-O(3)	×δ	2.840(3)	2.837(3)	2.833(3)	2.838(3)	2.888(3)	2.878(3)	2.847(3)	2.885(3)	2.816(3)	2.829(3)

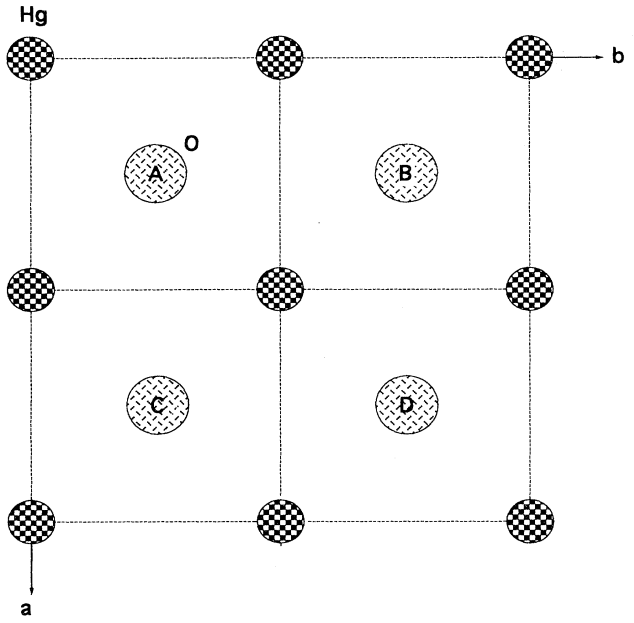

FIG. 3. HgO_δ plane in $HgBa_2CuO_{4+\delta}$. *A*, *B*, *C*, *D* identify the O(3) sites in this plane.

by 0.0091 and 0.0265 Å, respectively, as the temperature decreases from 296 to 10 K. The smooth variation of these quantities makes it evident there is no structural transition occurring as a function of temperature. It is interesting to note that the apical distance Cu-O(2) decreases significantly as the temperature decreases. Since the Hg-O(2) distance remains practically constant over the temperature range explored, it follows that the observed variation of the *c* axis with temperature is all reflected in the change of the Cu-O(2) apical distance. This behavior is in agreement with the results obtained by Wagner *et al.*,[3] but it is different from that observed in Hg1212 (Ref. 9) and Hg1223,[12] where a decrease of the Hg-O distance was observed with decreasing temperature, with little variation in the Cu-O apical distance.

The oxygen content δ in the material was varied from 0.04 to 0.23 via different annealing conditions. We first reduced the oxygen content by annealing in vacuum (*S*1-AV), and δ was reduced from 0.18 to 0.08, with a corresponding T_c of 53 K. The sample was then reannealed in O_2 (*S*1-RAO), and δ and T_c returned to 0.18 and 94 K, respectively. All the structural parameters also returned to those of the as-prepared sample, with most of the differences being within one standard deviation. Thus the variation in oxygen content is completely reversible. The room-temperature variations of *a*, *c*, and bond distances are shown in Fig. 5 as a function of the oxygen content δ. The *a* axis decreases smoothly and almost linearly as δ increases from 0.04 to 0.023. The *c* axis, on the other hand, initially increases with increasing oxygen content, and then decreases smoothly with further increase of δ. Just as with temperature, though, all the structural parameters vary smoothly with δ, indicating that there are no structural transitions occurring as the oxygen content changes.

We now turn our attention to some of the more subtle features of the analysis and structure. As shown in Table II, the temperature factors of some atoms are significantly larger than expected, in particular for the Hg, Ba, and O(2) sites. The large temperature factors could of course simply indicate a large thermal motion,

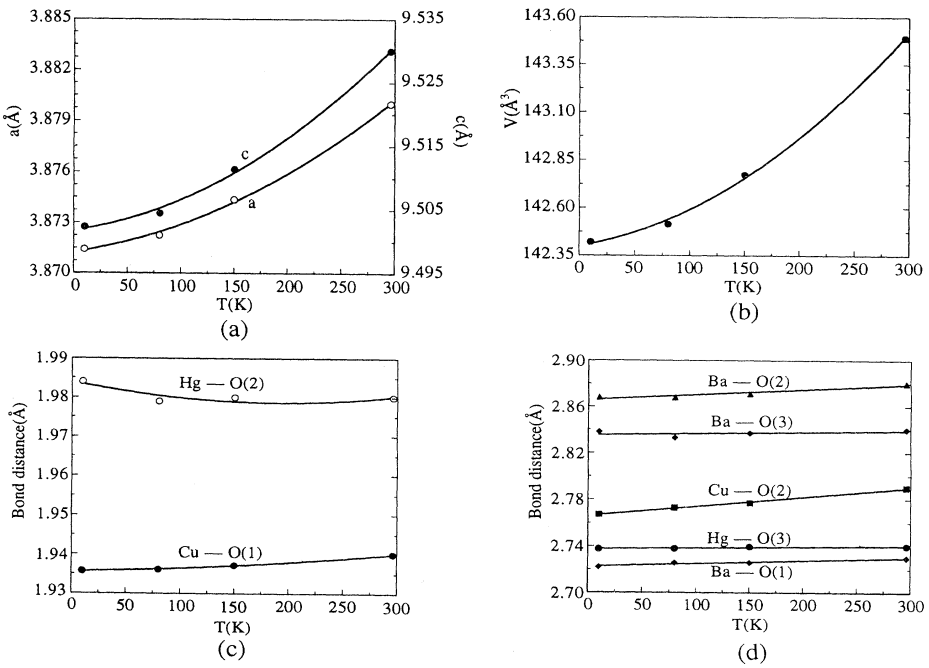

FIG. 4. (a) Lattice parameters, (b) unit-cell volume, and (c), (d) selected bond distances, as a function of temperature.

but they may also indicate a shift of the atomic position, some structural disorder in the position, or only partial occupation of the site. We thus carried out a number of additional refinements to investigate these possibilities.

One possible generalization is to allow the thermal displacements to have tetragonal symmetry (i.e., $B_{11}=B_{22}\neq B_{33}$) rather than being isotropic. We thus carried out refinements allowing anisotropic thermal factors for the Hg, Ba, and the O(2) sites, while also refining the occupancy factors. The results are given in Table IV. The refinements show that the mean-square displacements for the O(2) remained essentially isotropic. For the Ba ions they are also isotropic for the lowest oxygen concentration ($\delta=0.04$), but become anisotropic, with $B_{33}>B_{11}$, for larger δ. This may indicate a shift or disorder along the c axis, and we will return to this question below. The refinements indicate that both of these sites are fully occupied.

For the Hg the overall mean-square displacements determined from the fits are large and anisotropic, with $B_{11}>B_{33}$. This behavior was also observed in the higher-layer materials[9,12,14] and may be due to thermal motion or positional disordering. Since the O(3) sites on the Hg layers are partially occupied, we might imagine that the Hg occupy different positions depending on whether or not the O(3) sites are locally occupied. In the study of the Hg1212 system,[19] for example, the (apparent) thermal factor increased with increasing oxygen content, and was interpreted in terms of the degree of the disorder in the structure depending on the oxygen content. However, in the present analysis we do not find such a dependence on δ. In addition, attempts to shift the Hg from its ideal position (0,0,0) to (x,x,z) gave $x=0.00(2)$ and $z=0.01(4)$, and did not improve the agreement in the fit. These results indicate that if there is any positional disorder at all it is too small to be detected in the present powder-diffraction data.

Another possible interpretation of the large temperature factor of Hg is that the site is not fully occupied, or that some of the Hg ions have been replaced by another element (such as Cu) with a smaller scattering amplitude. The possible loss of Hg during the repeated sample annealings is a particular concern because of its high vapor pressure. Consider the possibility of Cu substitution on the Hg site. Since $b_{Cu}=0.77$ while $b_{vacancy}=0$, we would have to have 23% of the sites actually occupied by Cu to account for an apparent 9% Hg vacancy (see Table IV), for example. Since there was no significant weight loss during the initial sample preparation, and since both the Cu and Ba sites in the primary compound are fully occupied, we would then need 46% of the Ba in impurity phases, while in actuality any impurity phases constitute

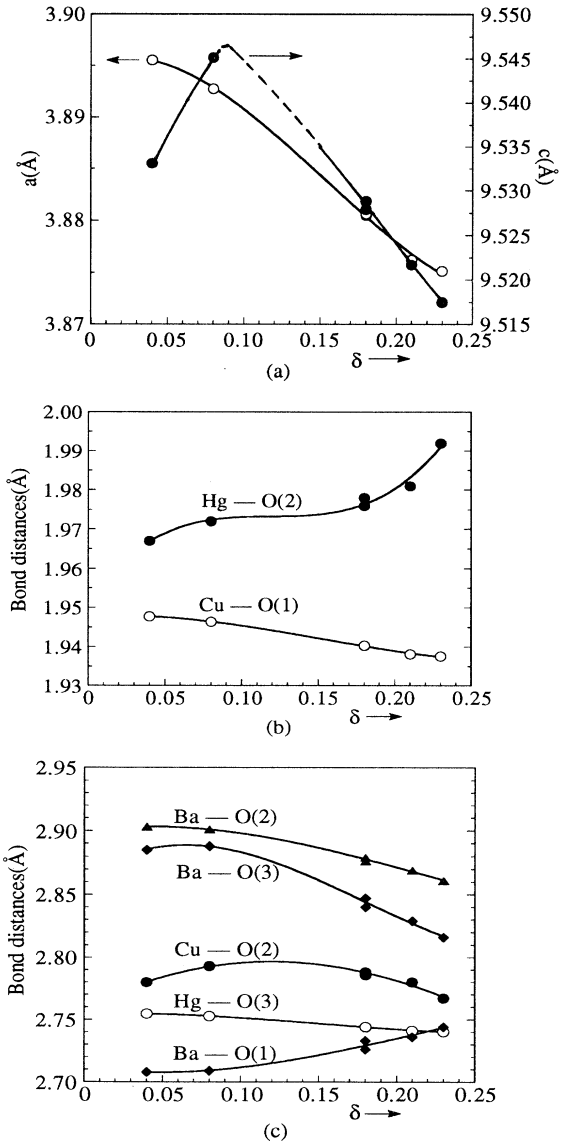

FIG. 5. (a) Lattice parameters, and (b), (c) selected bond distances, versus the oxygen content δ.

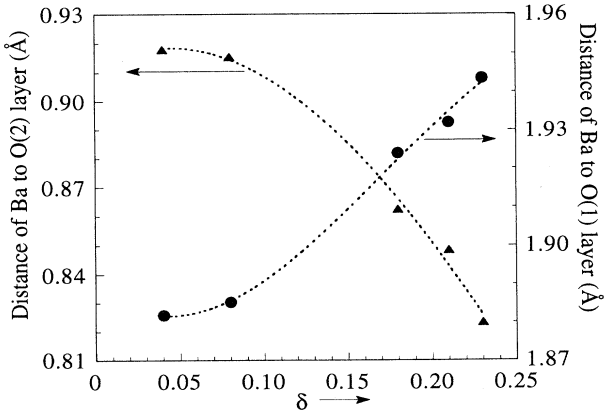

FIG. 6. Distance of the Ba ion (z coordinate) from the O(1) and O(2) planes of oxygen ions, showing that the Ba ion moves towards the O(3) site with increasing δ.

TABLE IV. (Top) Occupancy parameters of Hg (at room temperature). (Bottom) Anisotropic temperature factors of Ba ($B_{22}=B_{11}$) and Ba splitting into $[\frac{1}{2},\frac{1}{2},z(1)]$ and $[\frac{1}{2},\frac{1}{2},z(2)]$; constraints: $n_{Ba(2)}=n_{O(3)}=1-n_{Ba(1)}$, $B_{Ba(1)}=B_{Ba(2)}$ (at room temperature).

Sample label (δ)/[T_c (K)]	*S*1-AP (0.18)/(95)	*S*1-AV (0.08)/(53)	*S*1-RAO (0.18)/(94)	*S*1-RAV (0.04)/(0)	*S*2-PHP (0.21)/(80)	*S*1-RAOHP (0.23)/(30)
n	0.99(1)	0.97(1)	0.92(1)	0.95(1)	0.90(1)	0.91(1)
B (Å^2)	1.37(5)	1.15(7)	1.13(6)	1.07(6)	0.84(8)	1.12(6)

	Sample label (δ)/[T_c (K)]	*S*1-RAV (0.04)/(0)	*S*1-AV (0.08)/(53)	*S*1-AP (0.18)/(95)	*S*2-PHP (0.21)/(80)	*S*1-RAOHP (0.23)/(30)
		Anisotropic temperature factor				
	B_{11} (Å^2)	0.84(7)	0.50(8)	0.51(7)	0.5(1)	0.72(6)
	B_{33} (Å^2)	0.8(1)	0.9(1)	1.2(1)	1.0(1)	1.3(2)
	B_{33}/B_{11}	0.95	1.8	2.4	2.0	1.8
			Ba splitting			
Ba(1)	$z(1)$		0.3045(5)	0.3025(7)	0.3001(10)	0.3006(7)
	n		0.92(1)	0.83(1)	0.79(1)	0.77(1)
Ba(2)	$z(2)$		0.276(7)	0.275(3)	0.284(4)	0.281(2)
	n		0.08(1)	0.17(1)	0.21(1)	0.23(1)
	B (Å^2)		0.61(8)	0.59(6)	0.64(9)	0.57(6)

$<1.5\%$. We also did not find any significant changes in the intensities of the weak impurity peaks as a function of δ in all the samples involved in these experiments. Thus any possible Cu occupancy on the Hg sites is at the few percent level at most; we believe it is more likely that the true thermal displacements are large, or that there are some vacancies or small positional disorder on the Hg sites.

We now turn to the interesting situation of the Ba site. The data of Fig. 5(c) show that the Ba-O(2 or 3) distances decrease while the Ba-O(1) distance increases with increasing δ, which suggests that the Ba ions are shifting. Figure 6 shows more clearly that this is indeed the case. We see that the distance of the Ba ion from the O(2) plane decreases while the distance to the O(1) plane increases with increasing δ. This shift in the z coordinate is quite substantial (-0.100 and 0.065 Å, for the Ba$\rightarrow$O(2) plane and Ba$\rightarrow$O(1) plane, respectively), while the Ba-O(3) bond contracts $\sim$0.08 Å. Note in particular that these shifts are much larger than the overall contraction of c of only 0.028 Å over the range of δ explored.

Since the O(3) site in the structure is only partially occupied, one may speculate that the Ba atoms shift along the c axis when an O(3) ion is present, as shown in Fig. 7. We therefore refined a model with two Ba sites, Ba(1) at $[\frac{1}{2},\frac{1}{2},z(1)]$ and Ba(2) at $[\frac{1}{2},\frac{1}{2},z(2)]$. We also allowed the

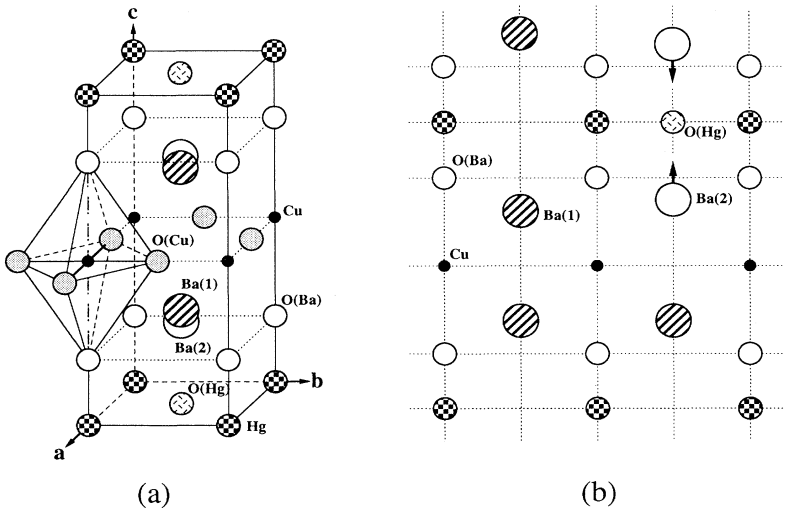

FIG. 7. (a) Two-site model [Ba(1) and Ba(2)] for the Ba ions in $HgBa_2CuO_{4+\delta}$; (b) the section of $a=1/2$ (or $b=1/2$). When the O(3) site is occupied the Ba moves away from the Cu layer and towards the Hg layer.

TABLE V. Valences (u.v.–unit valence) calculated from cation-oxygen bonds.

Sample label (δ)/[T_c (K)]	*S*1-RAV (0.04)/(0)	*S*1-AV (0.08)/(53)	*S*1-AP (0.18)/(95)	*S*2-PHP (0.21)/(80)	*S*1-RAOHP (0.23)/(30)
ΣV_{Hg} (u.v.)	1.827	1.824	1.836	1.836	1.795
ΣV_{Ba} (u.v.)	2.064	2.072	2.075	2.085	2.083
ΣV_{Cu} (u.v.)	2.036	2.040	2.075	2.088	2.094
$\Sigma V_{O(1)}$ (u.v.)	−2.259	−2.259	−2.195	−2.193	−2.166
$\Sigma V_{O(2)}$ (u.v.)	−1.719	−1.710	−1.749	−1.758	−1.755
$\Sigma V_{O(3)}$ (u.v.)	−0.831	−0.830	−0.896	−0.913	−0.931

Hg to shift if it wanted, but we found that there was no significant shifting for Hg away from the ideal position. However, we obtained significantly different $z(1)$ and $z(2)$, which were accompanied by smaller temperature factors as shown in Table IV (bottom). The only exception was for the $\delta=0.04$ sample, where the Ba yielded an almost isotropic thermal parameter. For this low occupancy the calculation with the two-site Ba model gave meaningless results.

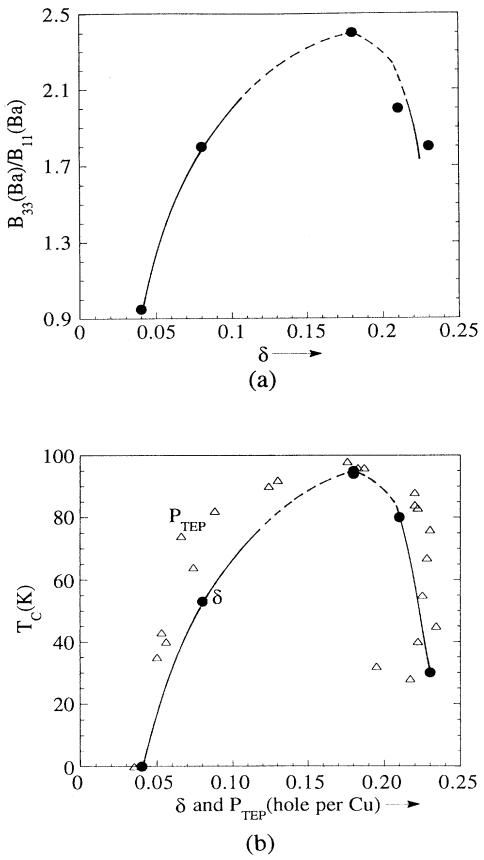

FIG. 8. (a) The ratio B_{33}(Ba)/B_{11}(Ba) plotted versus oxygen content δ. (b) The behavior of T_c vs δ and T_c vs hole concentration. The solid points are from this study, while the triangles are taken from Ref. 15. The solid curves are simply a guide to the eye for the neutron data; parabolic fits to the T_c vs hole concentration are given in Ref. 15.

Figure 8(a) shows the ratio of B_{33}/B_{11} for the Ba ion plotted as a function of δ. The increase in B_{33} which causes this behavior we interpret as the disorder and/or shift of the Ba when the O(3) site is occupied. There is clearly a strong variation, with a maximum at $\delta\approx0.18$ which is just at the maximum of $T_c(\delta)$. In fact, the behavior of B_{33}/B_{11} mirrors the entire $T_c(\delta)$ as shown in Fig. 8(b). Here the $T_c(\delta)$ data (solid points) are from this study, while the triangles are $T_c(P_{TEP})$, where P_{TEP} is the hole per Cu as determined by thermoelectric power measurements.[15] It is clear that the behavior of $T_c(P_{TEP})$ is very similar to $T_c(\delta)$. In the underdoped regime T_c decreases with decreasing δ, and T_c becomes 0 for $\delta\leq0.04$. This means that this material is not a self-doped superconductor, in contrast to an early suggestion.[20] In the overdoped region, T_c rapidly decreases from 95 to 30 K as δ increases from 0.18 to 0.23. Thermogravimetric measurements, however, indicate that there is more oxygen present in the sample than is observed at the O(3) site,[15] and this led to the speculation that another oxygen site was also occupied. However, in the present study we have not been able to detect such an extra oxygen site.

Finally we comment on the rate of doping caused by the insertion of O(3) in this system. One of the interesting points from these hole-doping studies,[15] as shown in Fig. 8(b), was that the doping level onto the Cu layer corresponds to only about one electron transferred per O(3) oxygen instead of the customary O^{2-}. This reduced doping has also been seen in band-structure calculations based on the local-density approximation, carried out to elucidate the effects of oxygen doping on Hg1223.[21] In the $HgBa_2Ca_{n-1}Cu_nO_{2n+2+\delta}$ series of superconductors, the CuO_2 planes are considered to be hole doped by the extra oxygen on the mercury layers. These additional oxygen atoms are strongly bound to the barium located on the nearest layers and this causes the barium to move away from the oxygen in the Cu layers and towards the Hg layer. The data of Fig. 8(a) clearly demonstrate that there is a direct relationship between the doping and the average movement of Ba as a function of δ. In Table V we present calculations of the formal valence values obtained with Brown's method of valence and/or distance relationships,[22] which tend to be accurate to 10–20%. It is very interesting to note that the valence on O(3) comes out to be just under one electron per ion, in agreement with experimental observation for this material.

ACKNOWLEDGMENTS

We would like to thank J. J. Rush and A. Santoro for helpful discussions and assistance. The research at the University of Houston is supported in part by the NSF, DMR 91-22043, USAFOSR Grant No. F49620-93-0310, the State of Texas through the Texas Center for Superconductivity at the University of Houston, and the T.L.L. Temple Foundation.

[1]S. N. Putilin, E. V. Antipov, O. Chmaissem, and M. Marezio, Nature (London) **362**, 226 (1993).

[2]L. Gao, Z. J. Huang, R. L. Meng, J. G. Lin, F. Chen, K. Beauvais, Y. Y. Xue, and C. W. Chu, Physica C **213**, 261 (1993).

[3]J. L. Wagner, P. G. Radaelli, D. G. Hinks, J. D. Jorgensen, J. F. Mitchell, B. Dabrowski, G. S. Knapp, and M. A. Beno, Physica C **210**, 447 (1993).

[4]O. Chmaissem, Q. Huang, S. N. Putilin, M. Marezio, and A. Santoro, Physica C **212**, 259 (1993).

[5]S. N. Putilin, I. Bryntse, and E. V. Antipov, Mater. Res. Bull. **26**, 1299 (1991).

[6]S. N. Putilin, E. V. Antipov, and M. Marezio, Physica C **212**, 266 (1993).

[7]A. Schilling, M. Cantoni, J. D. Gao, and H. R. Ott, Nature (London) **363**, 56 (1993).

[8]R. L. Meng, Y. Y. Sun, J. Kulik, F. Chen, Y. Y. Xue, and C. W. Chu, Physica C **214**, 307 (1993).

[9]Q. Huang, J. W. Lynn, R. L. Meng, and C. W. Chu, Physica C **218**, 356 (1993).

[10]E. V. Antipov, S. M. Loureiro, J. L. Tholence, J. J. Capponi, C. Chaillout, O. Chmaissem, Q. Huang, M. Marezio, S. N. Putilin, and A. Santoro, Physica C **217**, 253 (1993).

[11]E. V. Antipov, S. M. Loureiro, C. Chaillout, J. J. Capponi, P. Bordet, J. L. Tholence, S. N. Putilin, and M. Marezio, Physica C **215**, 1 (1993).

[12]O. Chmaissem, Q. Huang, E. V. Antipov, S. N. Putilin, M. Marezio, S. M. Loureiro, J. J. Capponi, J. L. Tholence, and A. Santoro, Physica C **217**, 265 (1993).

[13]L. Gao, Y. Y. Xue, F. Chen, Q. Xiong, R. L. Meng, D. Ramirez, C. W. Chu, J. H. Eggert, and H. K. Mao, Phys. Rev. B **50**, 4260 (1994). See also C. W. Chu, L. Gao, F. Chen, Z. J. Huang, R. L. Meng, and Y. Y. Xue, Nature (London) **365**, 323 (1993).

[14]Q. Huang, O. Chmaissem, J. J. Capponi, C. Chaillout, M. Marezio, J. L. Tholence, and A. Santoro, Physica C **227**, 1 (1994).

[15]Q. Xiong, Y. Y. Xue, Y. Cao, F. Chen, Y. Y. Sun, J. Gibson, C. W. Chu, L. M. Liu, and A. Jacobson, Phys. Rev. B **50**, 10 346 (1994).

[16]R. L. Meng, L. Beanvais, X. N. Zhang, Z. J. Huang, Y. Y. Sun, Y. Y. Xue, and C. W. Chu, Physica C **216**, 21 (1993).

[17]A. C. Larson and R. B. Von Dreele (unpublished).

[18]C. W. Chu (unpublished).

[19]P. G. Radaelli, J. L. Wagner, B. A. Hunter, M. A. Bano, G. S. Knapp, J. D. Jorgensen, and D. G. Hinks, Physica C **216**, 29 (1993).

[20]D. L. Novikov and A. J. Freeman, Physica C **212**, 233 (1993).

[21]D. J. Singh and W. E. Pickett, Phys. Rev. Lett. **73**, 476 (1994).

[22]I. D. Brown and K. K. Wu, Acta Crystallogr. B **32**, 1957 (1976); I. D. Brown and D. Altermatt, *ibid.* **41**, 244 (1985).